

Application Results of Newly Developed EAF Refractories

Atsushi TORIGOE*¹
Ryoma FUJIYOSHI*³

Hisashi TOMIYA*²
Hitoshi KUNII*⁴

Abstract

We will explain the characteristics of our newly developed EAF refractories using typical examples. By applying sidewall refractories with high corrosion resistance, HIDEN and EBT tube, bottom blowing nozzle, slide gate valve for tapping, ABB type bottom electrode in DC furnace, and high slaking resistant bricks for back lining. Our customers can improve refractory performance and operation efficiency.

1. Introduction

As is well known in the industry, there are two primary methods to produce steel products; blast furnace (BF) and electric arc furnace (EAF). In the BF process, pig iron is produced by reducing the raw materials of iron ore and coke. The pig iron is then de-carbonized by converter (Basic Oxygen Furnace) and further refined in a secondary process to produce a molten steel product. In the EAF process, molten steel is produced by melting the scrap by an arc generated from an electrode. The molten steel is then sent to secondary refining. The steel manufacturing process using a blast furnace is the mainstream worldwide today.

Iron ore and coal, the primary raw materials used in the BF and BOF have well developed resource and distribution systems which are necessary to supply them on a global scale. It is very suitable for a society with a large continuous steel demand. At the same time, the ratio of steel products made by EAF is increasing in our society, which is equipped with systems that can efficiently collect and recycle steel scrap. According to R. Waugh et al., the future steel demand and scrap generation suggests the EAF process will become the main method¹⁾.

In contrast, there is a report²⁾ that the BF will continue to be the mainstream in the future. This is because of the operational environment and efficiency of the BF has been greatly improved by technological development,

and the actual steel scrap supply is insufficient for steel demand. No one knows for sure if the EAF or BF system will be the mainstream of the future but approximately 70% of crude steel can be made in the United States by EAF. The EAF ratio will grow for mainly developed countries in the future. In the EAF, much innovation has been accomplished and the efficiency of operation has been improved^{3),4)}. In addition, new refractory technology has developed and contributed to the efficiency of operation^{5),6)}. In this report, we describe the recent development and the efficiency of operation by the application of our newly developed EAF refractories. These include sidewall refractories with high corrosion resistance; HIDEN, EBT tubes, bottom blowing nozzles, slide gate valves for tapping, ABB type bottom electrodes in DC furnace, and high slaking resistance bricks for the back lining.

2. High Corrosion Resistance Bricks for EAF Side Wall ; HIDEN

EAF treatment utilizes an exothermal reaction with oxidation of Fe by oxygen injection and increase in molten steel temperature generating FeO. While reduction of FeO is performed by injection of carbonaceous materials, the slag contains relatively higher FeO. EAF steels are generally treated by the refining process in the EAF and the refining slag is also highly erosive. In addition, excessive increase in molten steel temperatures at "hotspots" increase the wear rate of the bricks due to the increase in

*¹ General Manager, Shaped Refractories R&D Sec., Research Dept. No.1, Research Center

*² Assistant Manager, Technical Sec., Okayama Plant, West Japan Works

*³ Shaped Refractories R&D Sec., Research Dept. No.1, Research Center

*⁴ Staff Manager, Technical Sec., Yumoto Plant, East Japan Works

the reaction velocity and thin coating layer on the brick surface by the viscosity drop in the slag. In such case, MgO-C brick with corrosion resistance is applied as the EAF side wall refractory because the damage factor is mainly erosion by slag.

The corrosion resistance of the MgO-C brick has been improved by use of high purity raw materials and densification by adjusting the metal addition. In contrast, Umeda and et.al.⁷⁾ paid close attention to the influence of the heat load received from the exposed BOF MgO-C bricks and examined the effect of cyclic thermal treatment on the corrosion resistance of the samples. As a result, erosion was markedly enhanced by cyclic thermal treatment and deterioration of the structure progressed by heating. This concept was similar to an EAF and it was thought that restraint of deterioration of brick texture by cyclic thermal treatment would be effective for reducing the wear rate. Deterioration of the MgO-C brick occurs through the progression of the MgO-C reaction as shown in Eq.(1).



Carniglia⁸⁾ examined the reaction in Eq.(1) using a BOF brick in detail and stated that the rate-determining step is the diffusion of the gas formed by this reaction to the brick structure. According to this knowledge, deterioration of brick structure is controlled by reducing

the diffusion speed of Mg(g) in the brick and can reduce the wear rate. Based on this assumption, we examined the particle size and manufacturing process of the brick, and controlled the diffusion of Mg(g) by making a dense brick texture. As a result, we have developed low porosity MgO-C bricks called "HIDEN".

Figure 1 shows the apparent porosities of HIDEN and conventional products. Apparent porosity of the products (200°C ≧) is equal, but after heating to 1000°C and 1500°C the porosity of HIDEN is small. Figure 2 shows the erosion test result of MgO-C brick samples that changed in porosity after firing. Raw materials of same purity were used with various particle sizes and manufacturing methods. The erosion index is proportional to porosity after firing.

We evaluated HIDEN indicating such a characteristic at actual EAF. Figure 3 shows the test results, the HIDEN installed area clearly protrudes. Figure 4 shows the microstructure after use of HIDEN and conventional products. In the HIDEN specimen, the embrittled layer at the hot face was thin, as we were able to confirm an embrittlement suppressant effect even after use.

Due to the HIDEN high corrosion resistance with a minimized metal addition, the rise in modulus of elasticity after heating is low and the risk of spalling is less, thus, we can expect better corrosion-resistance and further improvement by decreasing the carbon content. As

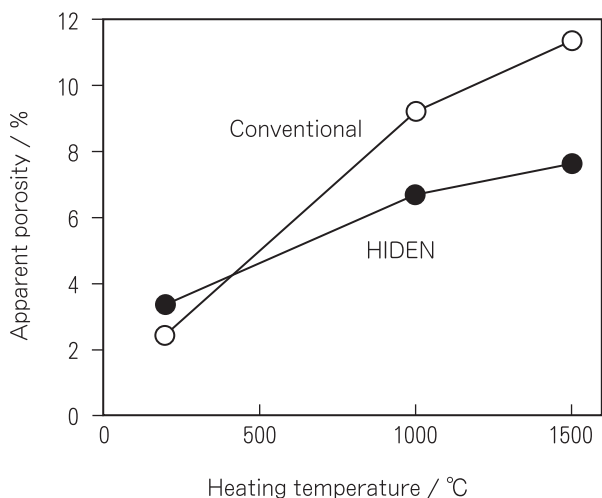


Fig.1 Comparison of apparent porosity variation of HIDEN and conventional MgO-C brick as a function of heating temperature.

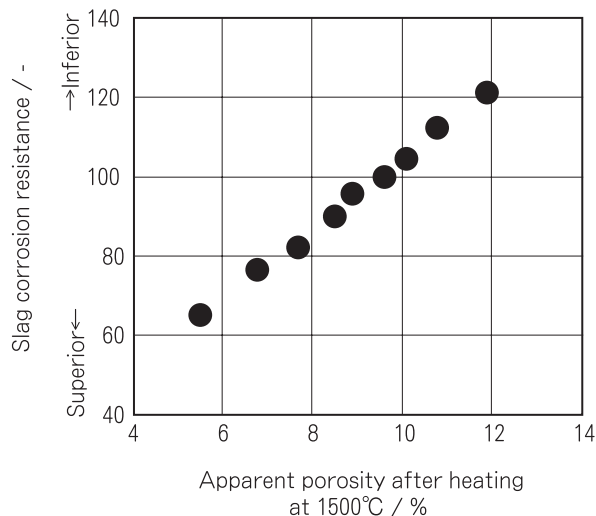


Fig.2 Variation of MgO-C Brick corrosion resistance as a function of apparent porosity after heating.

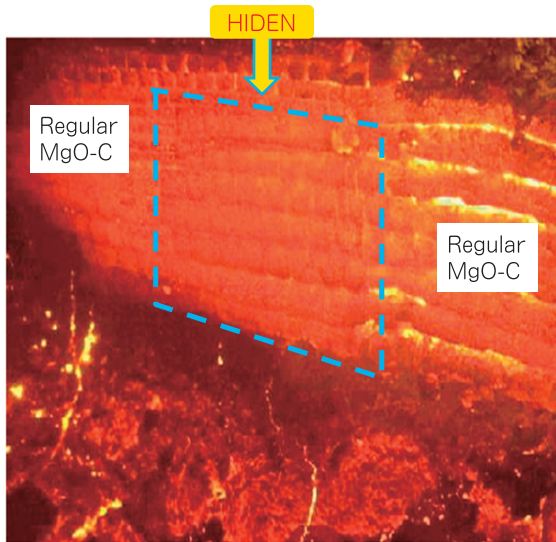


Fig.3 Wear status of HIDEN and reguar MgO-C brick of an EAF.

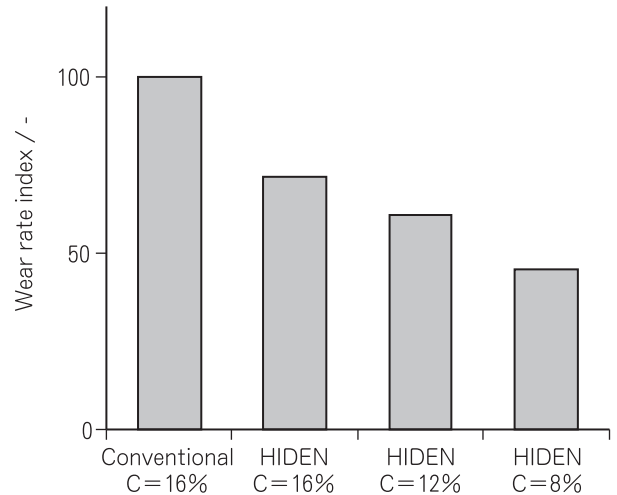


Fig.5 Influence of carbon fraction of HIDEN on wear rate of an EAF.

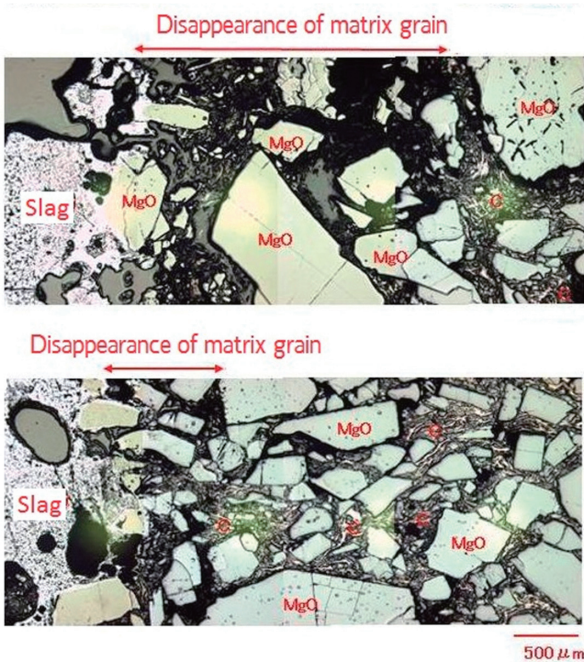
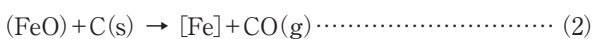


Fig.4 Microstructures of HIDEN and conventional MgO-C brick after use.

mentioned above, there is a significant amount of FeO in EAF slag. For this reason the erosion speed of low carbon type HIDEN decreases since the C contained in MgO-C brick disappears by the reaction of liquid phase oxidation as shown in Eq.(2).



Therefore, in an EAF where HIDEN was applied, we performed a test to reduce the carbon gradually while observing for any cracks and/or spalling. The reason was that there was no cracking or spalling even when we reduced the carbon of HIDEN in this EAF. HIDEN was able to reduce the wear rate as shown in Fig.5. The wear speed of the EAF sidewall was decreased by applying the MgO-C brick HIDEN with a controlled embrittlement layer and ultimately overall brick structure, improving the EAF operation by extending the campaign life. After applying standard HIDEN in an actual furnace we saw improvement, so we expect even better EAF productivity when we fine tune the materials while observing their use in operation.

3. EBT Tube Refractories

As for EAF to ladle tapping systems, there are tilting spouts and bottom tapping types. There are Concentric Bottom Tapping (CBT) and Eccentric Bottom Tapping (EBT), and EBT systems that have begun to expand. Figure 6 shows an installation image of EBT. An application of EBT allows the expansion of the water cooling area, decreases the refractories cost and the discharge quantity of the slag into ladle, improving the quality of the steel. The operation efficiency was also improved by shortening the tapping time³⁾. Cylindrical refractories are applied to the steel taphole that are called EBT tubes. MgO-C bricks are usually used in the EBT tubes, in which the bricks are placed on top of one another to form

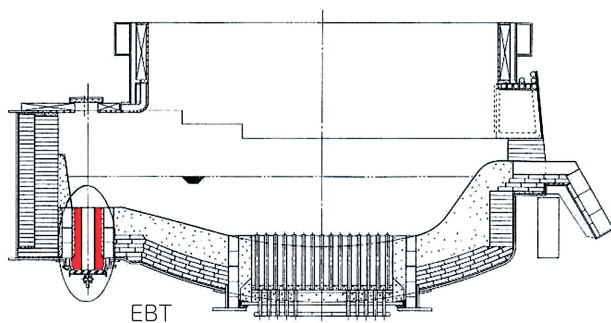


Fig.6 Schematic image of EAF equipped with EBT.

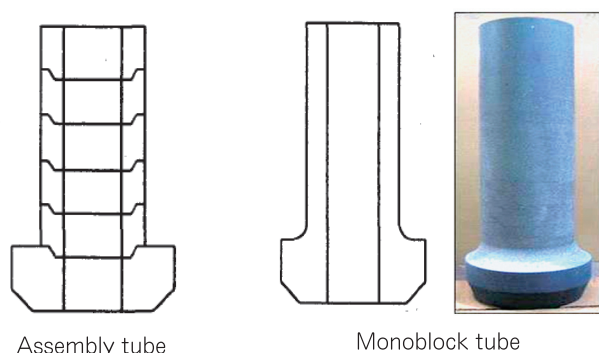


Fig.7 Assembled EBT tube and monoblock EBT tube.

a ring. We have adopted the monoblock tube because clogging of filling sand in the joint can lead to bridging causing opening failure. The upper bricks are at risk of floating when the damage starts from the joint area (Fig.7).

When tapping the furnace repeatedly, the EBT tube gradually wears and the inside diameter of tube increases, so it is changed regularly. It is preferable to synchronize the timing of the exchange with the timing of EAF maintenance. Therefore the initial inside diameter of the EBT tube is determined from the wear rate and the exchange timing according to the inside diameter. As a result the tapping time is longer with the small inside diameter of the EBT in the early stages, and operation efficiency lowers. In other words, the initial inside diameter can be increased by using an EBT tube with a low wear rate and improve operation efficiency of EAF.

As for the wear mechanism of the EBT tube, abrasion by the flow rate of molten steel and erosion by slag inclusions

Table 1 Typical qualities of MgO-C and Al_2O_3 -MgO-C for EAF

	MgO-C	MgO-C	Al_2O_3 -MgO-C
	C=20%	C=12%	C=9%
After drying			
Apparent porosity / %	3.7	4.2	4.6
Bulk density / -	2.81	3.02	3.06
Cold crushing strength / MPa	34	39	63
After fired at 1500°C for 3h			
Apparent porosity / %	11.4	9.5	8.8
Bulk density / -	2.72	2.97	3.01
Cold crushing strength / MPa	25	31	49
Hot modulus of rupture at 1400 / MPa	10.3	12.4	15.7

in the tapping steel is important. There are many refining treatments in EAF operations according to steel class, and one of them is low basicity slag composition. In addition, there may be a high occurrence of thermal spalling in an EBT tube depending upon operation and structure. We have a line-up of some materials to support such various cases. Table 1 shows the standard quality of 3 representative materials. All materials are high density bricks with high corrosion and abrasion resistance; (A) quantity of carbon 20% with general versatility, and (B) reduced carbon content with high abrasion resistance and high strength, for use in an EAF where the effect of spalling is small, (C) Low C Al_2O_3 -MgO-C materials used for an EAF operating with low slag basicity and shows high abrasion resistance.

Figure 8 shows the abrasion test results of (A)-(C). All samples show high abrasion resistance, and in the low carbon materials abrasion resistance is better. Figure 9 shows the relationship between wear rate of EBT tube at EAF with low basicity operation and laboratory abrasion index of (A)-(C). The wear rate decreases in proportion to an abrasion index, and the correlation between EBT tubes wear rate and abrasion resistance is high. As shown in Fig.10, our EBT tube maintains a good texture and properties even after use. By applying (C) in this EAF, we were able to extend the initial diameter of EBT in the early stages, and improve the operation rate by shortening the tapping time just after the EBT exchange.

In this way, we can improve the wear rate by making the materials of the EBT tube wear in coordination with the operation of EAF. If wear rate can be decreased, we



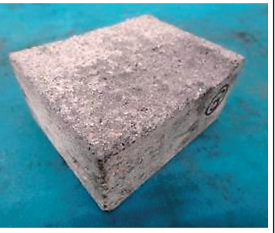

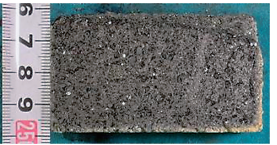

	(A) MgO-C (C=20%)	(B)MgO-C (C=12%)	(C) Al ₂ O ₃ -MgO-C(C=9%)
Appearance			
Cut surface			
Abrasion index	100	86	59

Fig.8 Abrasion test results of bricks for EBT tube.

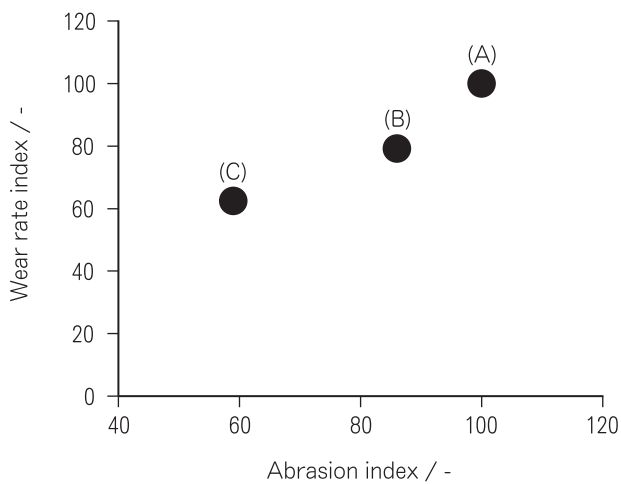


Fig.9 Variation of wear rate of EBT tube as a function of abrasion index obtained from an EAF which operates with low basicity slag.



(C) C=9% Al₂O₃-MgO-C bricks

	Apparent porosity / %	Bulk density / -
a	8.5	3.02
b	8.7	3.00
c	9.0	2.99

Fig.10 Cut surface and properties of the EBT tube after used for 90heats.

are able to increase the initial diameter with the aim life and contribute to improving the operation rate of the EAF.

4. Bottom Blowing Refractories for EAF

Blowing can improve the refining process of molten steel stirring, reduce occurrences of undissolved scrap, improve alloy yield ratio, reduce electric power consumption, and shorten the operation time^{(4),(9)-(14)}. Inert gas

blowing during bottom EAF treatment is particularly effective for producing high grade stainless and specialty steel. Figure 11 shows the effect of bottom blowing as shown by Fukumoto and others⁽⁹⁾. The preferential oxidation of [C] occurs because of gas blowing, and shows that Cr yield improves. Gas blowing is performed using the Multi-Hole Plug (MHP) where a large number of stainless steel narrow tubes are arranged in MgO-C brick.

Figure 12 shows the standard damage and basic

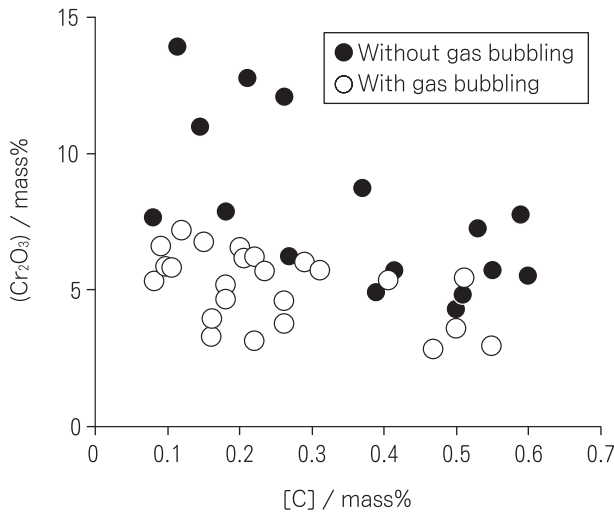


Fig.11 Variation of (Cr_2O_3) as a function of $[C]$.

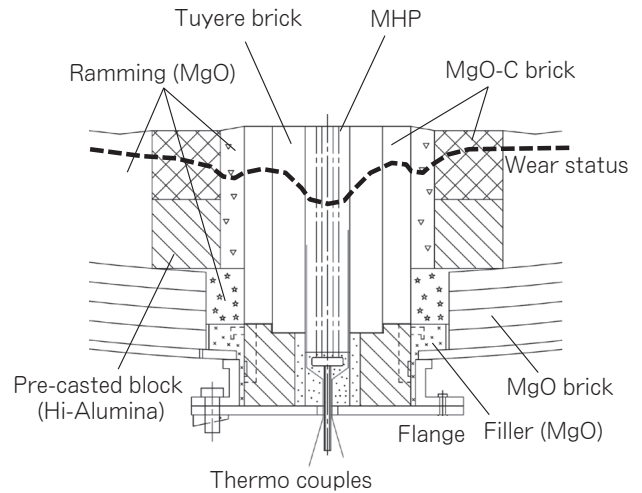


Fig.12 Basic design and typical wear status for bottom blowing refractories.

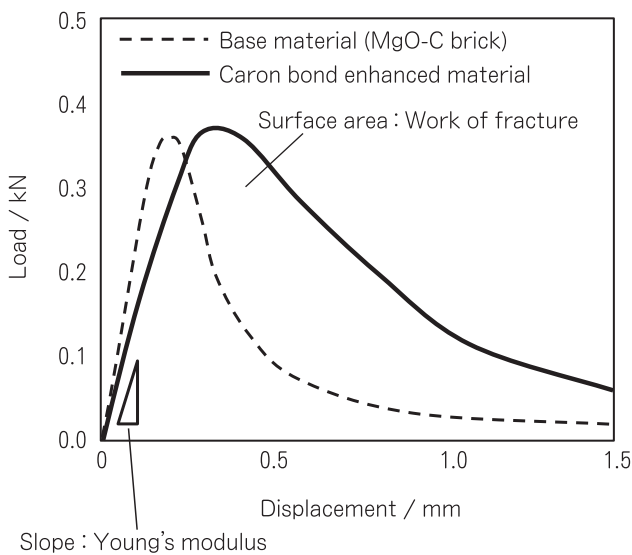


Fig.13 Effect of carbon bond enhancement on work of fracture.

structure of bottom blowing refractories. As shown in the heavy dotted curve in Fig.12, that damage occurred partially due to abrasion and thermal spalling in the MHP area for gas blowing. Abrasion occurs because of the violent turbulence of molten steel suspending carbonaceous material and refining agent at the gas blowing part. It is thought that the abrasion is a grand total of the micro fractures resulting from fine crack initiations and propagations caused by the collision of particles¹⁵⁾.

Thermal spalling is caused by strong thermal stress

occurring from the cooling caused by the inert gas. Thermal spalling is a phenomenon occurring when the stress is caused by a difference of the distortion quantity over a difference in temperature, and exceeding the fracture strength of the bricks. This stress σ , difference of strain $\Delta \epsilon$, the modulus of elasticity of bricks E is expressed as Eq.(3).

$$\sigma = \Delta \epsilon \cdot E \dots\dots\dots (3)$$

When such bottom blowing bricks wear is indicated, application of high abrasion resistant MgO-C brick with strengthened carbon bond is effective. This is due to the reinforcement of the carbon bond reducing the modulus of elasticity of the materials, and it increases the work of fracture. Figure 13 shows the plotted load and the displacement of the sample in the bending test. The early degree of inclination in this figure is equivalent to the modulus of elasticity, and the maximum load supports the fracture strength. A crack occurs with the maximum load. In addition, the area of the part surrounded in a plot supports the work of fracture consumed by the destruction of the sample, and the area after the maximum load showed the work consumed to propagate the crack. As shown in Fig.13, the reinforcement of the carbon bond is effective for increasing the work of fracture and drop in the modulus of elasticity, particularly the increase in the work of fracture is consumed from the propagation of crack. As shown in Eq.(3), the reduction in the modulus of elasticity reduces thermal stress, and raises resistance

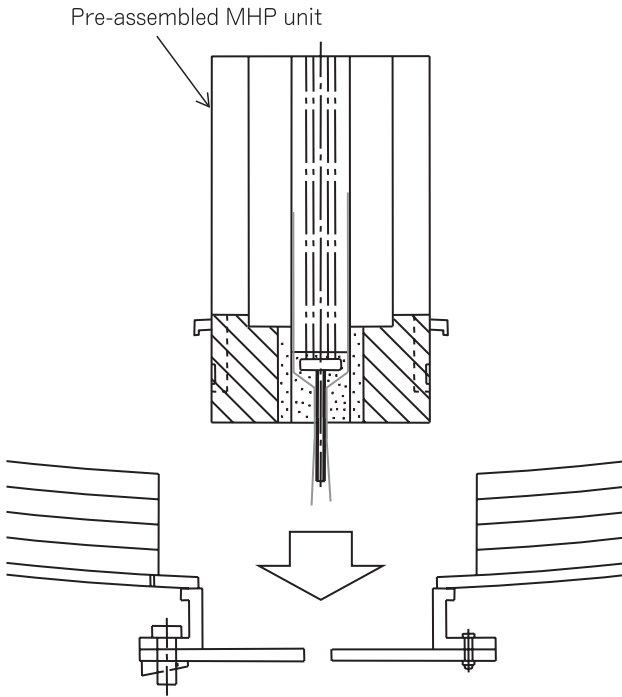


Fig.14 Installation of Pre-assembled MHP unit to EAF bottom.

for the generation of the crack. Improvement of the work of fracture raises the resistance for crack propagation. In this way, by reinforcement of the carbon bond, we can improve the abrasion and spalling resistance.

The thermocouple shown in Fig.12 performs the role of backup sensor, to prevent the leakage of molten steel

by stopping gas blowing when the thermocouple reaches a set point, then repairs can be made. In Fig.12, we can remove MHP after use, by opening a flange at the lower part. In addition, as shown in Fig.14, installation is easy using a hanging jig because the MHP unit is a monoblock structure comprised of a MHP and tuyere brick.

As mentioned above, MgO-C brick which is superior in thermal spalling and abrasion resistance is used for the MHP unit, but local erosion of the gas blowing area cannot be avoided. Therefore we developed a combination tuyere system¹⁴⁾. Figure 15 shows a summary of the combination tuyere. The combination tuyere uses two tuyeres in a pair and the stainless pipes are set buried in the second tuyere. When they operate in this condition, tuyere #1 is initially used until #2 tuyere wears sufficiently to expose the stainless pipes. When the wear reaches the stainless tubes buried in the second tuyere exposed to bath level, gas blowing starts. Gas blowing starting of the second tuyere is also regard as sensor of the remaining thickness. At this time, gas blowing of first tuyere stops and repairing begins. After repairs, we can continue to use the #2 tuyere until the remaining material of the second tuyere reaches the management value. In this way, the combination tuyere system uses the partial damage of the tuyere effectively to extend the life of the bottom.

In the EAF, there is AC-EAF producing an arc between three movable electrodes and scrap or molten steel with a three-phase AC current. DC-EAF produces an arc between an anode bottom electrode and upper

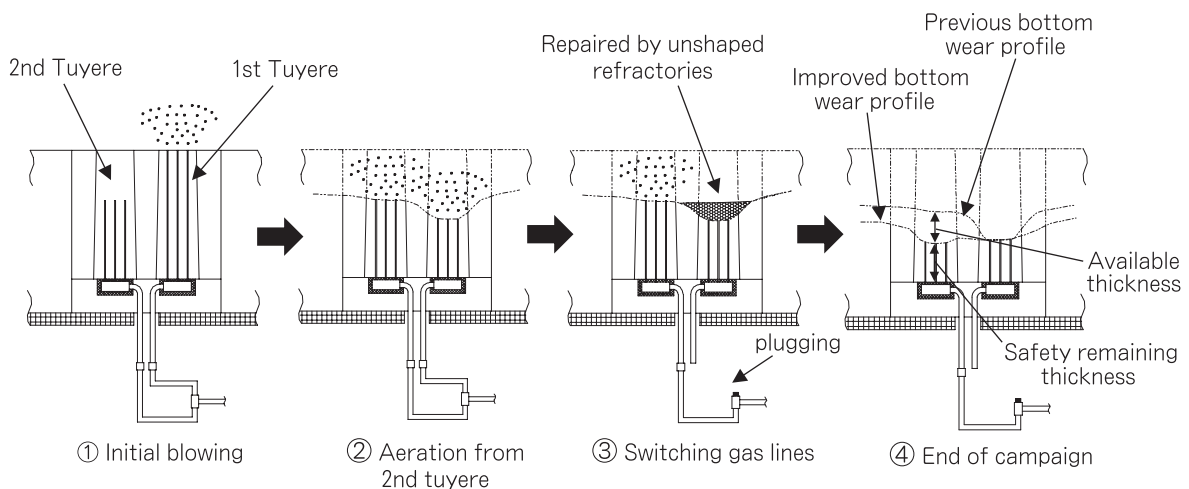


Fig.15 Schematic illustration of application of combination tuyere.

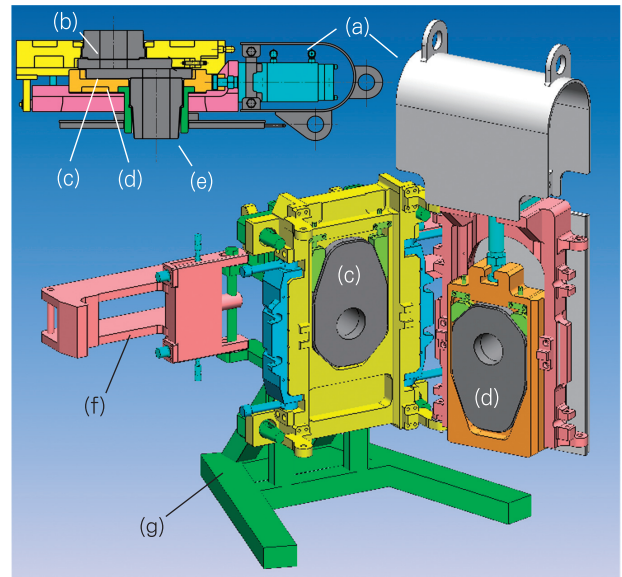
cathode movable electrode through the scrap or molten steel with direct current (DC).

A magnetic field is produced in a DC-EAF due to the electric current, and it is said that the bottom blowing does not generally perform well due to the existence of stirring by electromagnetic force³⁾, but there is a report that states that it is effective for the resolution of inactive regions by stirring the molten steel around the bottom¹³⁾.

5. Slide Gate Valve for EAF Tapping¹⁶⁾

When tapping from EAF to ladle at the final stage, there is some possibility of slag contamination into the ladle. In contrast, the large quantity of slag contamination can be reduced by applying the slide gate valve (SGV). This permits improvement of the second refinement efficiency and steel quality control. As shown in Fig.16, our SGV system can be easily mounted and removed.

Figure 17 summarizes our SGV system. Our SVG system is the same structure used for continuous casting, and consists of an upper nozzle, a top plate, a lower plate, and a lower nozzle. The upper nozzle connects with the tapping hole, and molten steel is drained from the lower nozzle to the steel ladle. The opening and shutting of the valve is carried out by sliding plate. The plate used for the SGV of the EAF consists of an inner ring and outer part made from two separate materials as shown in Fig.18.



(a)	SGV system
(b)	Upper nozzle
(c)	Upper plate
(d)	Lower plate
(e)	Lower nozzle
(f)	Cramp arm
(g)	Maintenance stand

Fig.17 Schematic images of SGV system set on the maintenance stand.

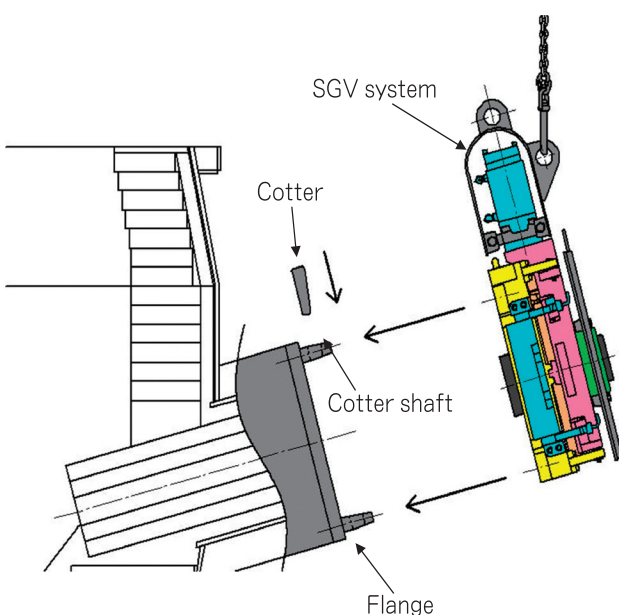


Fig.16 Installation of SGV system to the spout of EAF.

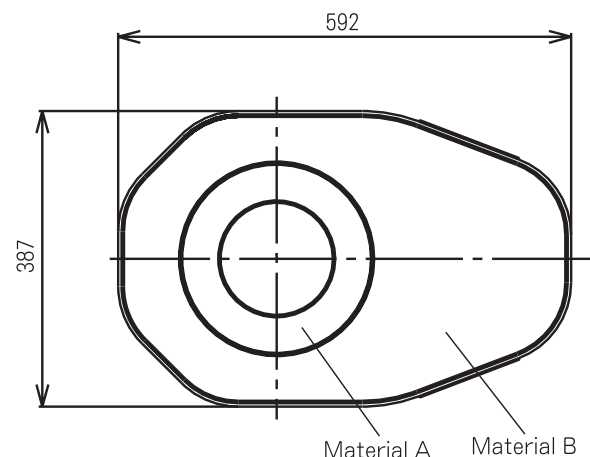


Fig.18 Refractory brick for plate of SGV system for EAF spout.

Table 2 Refractory materials for SGV system

Parts	Material
Upper nozzle	MgO-C
Plate material A	ZrO ₂
Plate material B	Al ₂ O ₃
Lower nozzle	Al ₂ O ₃ -C

Table 2 shows the summary of the materials for the SGV system. The upper nozzle uses MgO-C materials with high corrosion resistance and the lower nozzle uses Al₂O₃-C materials with high thermal spalling resistance. As for the plate ring, ZrO₂ materials with high corrosion resistance are used to reduce enlargement of the bore by erosion. The outer part is made of high Al₂O₃ materials with high heat resistance.

We confirmed safe and efficient installation and disassembly work of the SGV system at the EAF, and plate/nozzle exchange of an installed SGV system is possible as well. Spout tapping and bottom tapping is also possible with this system.

6. MgO-C Bricks for ABB Type DC-EAF Bottom Electrode¹⁷⁾

Up to now most of operating EAF was AC-EAF. But in DC-EAF, the consumption rate of electric power, electrode and refractories is less than AC-EAF, and there are characteristic of less noise and flicker so nowadays DC-EAF has been widely applied³⁾. The bottom electrode

for anode DC-EAF can be roughly classified into three types CLECIM-IRSID type, MAN-GHH type and ABB type. The ABB type utilizes conductive refractories as a bottom electrode whereas CLECIM-IRSID and MAN-GHH type use steel pins combined with refractories for the bottom electrode. We have developed MgO-C bricks which have high durability and conductivity for ABB type bottom electrodes¹⁰⁾.

Bottom electrode bricks play a role as the electrode itself. Due to electricity loss occurring if the electrical resistance of the brick is large, it is desirable for small electrical resistance levels. As a matter of course, superior durability is preferable. In cases where we checked the electrode brick during dismantling, metal penetration had occurred at the joint of the bricks and sometimes spalling was seen at the refractory hot faces during the skull removal. We estimate that these main damage factors arise from brick joints opening during heating and cooling. Therefore, reduction in brick shrinkage by a moderate residual expansion is important to improve the durability of the electrode brick.

The brick for our ABB type bottom electrodes shows low electrical resistance from low temperature to high temperature (Fig.19) and low thermal expansion and high residual expansion (Fig.20). Figure 21 shows the actual test results of our developed products having

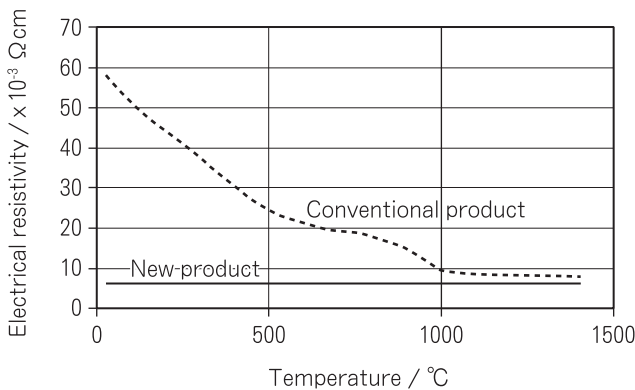


Fig.19 Electric specific resistances of MgO-C bricks for bottom anode of ABB type DC-EAF.

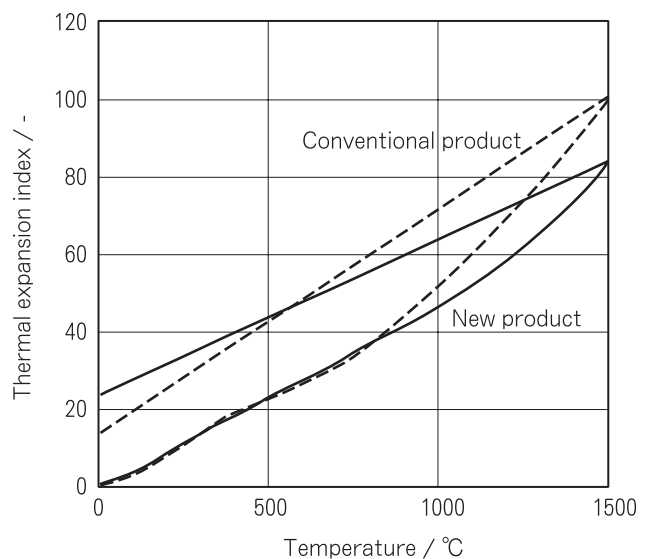


Fig.20 Thermal expansion behaviors of MgO-C bricks for bottom anode of ABB type DC-EAF.

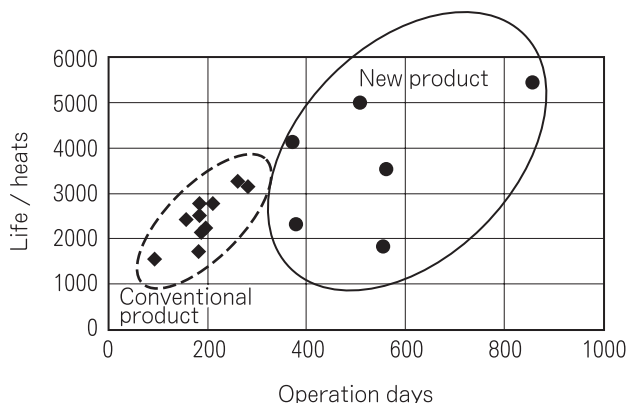


Fig.21 Service life of an of ABB type DC-EAF.

these properties. The developed product enables stable operation by the superior characteristic and greatly contributes to the life improvement for the ABB type bottom electrode.

7. High Slaking Resistance MgO Bricks for Permanent Lining

As shown in Fig.12, burned MgO bricks have been widely used for permanent bricks of EAF. Permanent brick need to have a stable minimum performance for a long term without deterioration in order to prevent EAFs from steel leakage even if the local erosion and partial loss of the working bricks. Taking the erosive qualities of the EAF slag aforementioned in section 2 into account, MgO brick have been used due to their high heat and corrosion resistance, and good resistance to alkali gas erosion. However, MgO forms a hydrate in a reaction with water according to Eq.(4).



So there is the disadvantage of a slaking phenomenon causing collapse by volume expansion.

Particularly, the EAF sidewall is cooled by a water-cooling jacket and is at risk of water leaks. In addition, sometimes a customer sprinkles water into the furnace for cooling purposes. Herewith, slaking of MgO bricks occurs and there is a possibility of failure.

In contrast, we have developed extremely high slaking resistant MgO brick. Table 3 shows the representative quality, and slaking test results using an autoclave

Table 3 Typical qualities of magnesia bricks with high slaking resistance

	Conventional	High slaking resistance
Chemical composition /mass%		
MgO	93.5	93.1
SiO ₂	2.0	2.0
Fe ₂ O ₃	0.8	0.8
Al ₂ O ₃	1.0	1.0
CaO	1.6	1.6
Apparent porosity /%	19.0	19.1
Bulk density /-	2.85	2.85
Cold crushing strength /MPa	57	60

	Conventional products	High slaking resistance products
Before test		
After autoclave test 0.3MPa-3h		
Weight change (%)	+5.4	+0.1

Fig.22 Autoclave test results of magnesia bricks.

shown in Fig.22. The chemical compositions and quality properties of high slaking resistant MgO bricks and conventional products are almost equal but the new products have excellent slaking resistance. A hydration reaction caused by water entering the furnace during repairs or from the water leaks can be reduced by utilizing this new product. In addition, the brick embrittlement due to slaking gradually occurs over a period of time may be difficult to detect. Therefore, this new product can contribute to reducing furnace repair time and reduction in the renewal of the permanent lining.

8. Conclusion

We are continuously developing various superior bricks for the EAF which can directly contribute to the

extension of life and improving efficiency of furnace operation. From this period, our focus is to develop the products in accordance with an operating condition of each EAF, continuously improving operation efficiency.

References

- 1) R. Waugh : Ironmaking & Steelmaking, **43** [4] 258-263 (2016).
- 2) D. Collins : Ironmaking & Steelmaking, **43** [4] 252-257 (2016).
- 3) T. Noda and K. Izumi : Tetsu-to-Hagané, **77** [6] 723-734 (1991).
- 4) G. A. Irons : Iron & Steel Technology, **2** [7] 110-122 (2005).
- 5) A. Hanna and K. Zettl : AISTech 2014 Proceedings, Association for Iron & Steel Technology, (2014).
- 6) G. Buchebner, A. Hanna and K. Zettl : AISTech 2014 Proceedings, Association for Iron & Steel Technology, (2014).
- 7) S. Umeda, T. Ikemoto, and T. Matsui : Taikabutsu, **59** [10] 544-551 (2007).
- 8) S.C. Carniglia : American Ceramic Society Bulletin, **52** [2] 160-165 (1973).
- 9) I. Fukumoto, K. Takami, T. Irie and K. Kawakami, Tetsu-to-Hagané, **78**, T161-164, (1992).
- 10) M. Uemura, H. Nabeshima, T. Ishiguro, H. Kato, I. Oyamada, Tetsu-to-Hagané, **78**, T189-192, (1992).
- 11) B. Li : ISIJ Int., **40**, 853-869 (2000).
- 12) S. Saito, H. Yamazoe, AISTech 2014 Proceedings, Association for Iron & Steel Technology, (2014), pp.1343-1352.
- 13) M. Ramírez, J. Alexis, G. Trapaga, P. Jönsson, J. Mckelliget, ISIJ Int., **41**, 1146-1155 (2001).
- 14) S. Imai, M. Takai, Shinagawa Technical Report, **55** 47-52 (2012).
- 15) R. Fujiyoshi, M. Iida, A. Iida, A. Torigoe, H. Yoshioka : Dai 4 kai Tekkou-you Taikabutsu Senmon Iinkai Hokokushu, Technical Association of Refractories Japan, (2016) pp.1-7.
- 16) A. Takata, K. Yamamoto, T. Saeki, M. Kajimura : Shinagawa Technical Report, **55** 41-46 (2012).
- 17) Y. Hanafusa, H. Tomiya, K. Mori : Shinagawa Technical Report, **59** 127-131 (2016).